Organic vapors from wood, straw, cow dung, and coal burning using Vocus PTR-TOF

Tiantian Wang[1], Jun Zhang[1], Houssni Lamkaddam[1], Kun Li[1, a], Ka Yuen Cheung[1], Lisa Kattner[1], Erlend Gammelsæter[1, b], Michael Bauer[1], Zachary C.J. Decker [1, c, d], Deepika Bhattu[2], Rujin Huang[3], Rob L. Modini[1], Jay G. Slowik[1], Imad El Haddad[1], Andre S. H. Prevot[1, *], David M. Bell[1, *]

1 Laboratory of Atmospheric Chemistry, Paul Scherrer Institute, Villigen, 5232, Switzerland

2 Department of Civil and Infrastructure Engineering, Indian Institute of Technology Jodhpur, 342037, India

3 Institute of Earth Environment, Chinese Academy of Sciences, Xian 710061, China

a now at: Environmental Research Institute, Shandong University, Qingdao, 266237, China

b now at: Department of Chemistry, Norwegian University of Science and Technology, Trondheim, 7491, Norway

c now at: NOAA Chemical Sciences Laboratory (CSL), Boulder, CO 80305, USA

d now at: Cooperative Institute for Research in Environmental Sciences, University of Colorado Boulder, Boulder, CO 80309, USA

Correspondence to: Andre S. H. Prevot (andre.prevot@psi.ch) and David M. Bell (david.bell@psi.ch)

Abstract

Solid fuel (SF) combustions, including coal and biomass, are important sources of pollutants in the particle and gas phase and therefore have significant implications for air quality, climate, and human health. In this study, we systematically examined real-time gas-phase emissions using the Vocus proton-transfer-reaction time-of-flight mass spectrometer, from a variety of solid fuels, including beech logs, spruce and pine logs, spruce and pine branches and needles, straw, cow dung, and coal. The average emission factors (EFs) for organic gases ranged from 6.7 to 74.2 g kg^{-1}, depending on the combustion phases and fuel types. Despite slight differences in modified combustion efficiency (MCE) for some experiments, increasing EFs for primary organic gases were observed with lower MCE. The $C_xH_yO_z$ family is the most abundant group, but a greater contribution of nitrogen-containing species and C_xH_y families (related to polycyclic aromatic hydrocarbons) could be found in cow dung burning and coal burning, respectively. Intermediate volatility organic compounds (IVOCs) also constituted a considerable fraction in solid-fuel combustions (from 12.6% to 39.3%), especially for spruce and pine branches and needles (39.3%), and coal (31.1%). Despite the large variability of EFs in the organic gas emissions, the relative contribution of different classes showed large similarities between the combustion phases in beech stove burning. The product from pyrolysis of coniferyl-type lignin and the extract of cedar pine needle were identified as characteristic compounds in the spruce and pine branches and needles open burning (e.g., $C_{10}H_{14}O_2$, $C_{11}H_{14}O_2$, $C_{10}H_{10}O_2$). The characteristic product ($C_9H_{12}O$) from the pyrolysis of beech lignin was identified as the characteristic compound for beech log stove burning. Many series of nitrogen-containing homologues (e.g., $C_{10}H_{11-21}NO$, $C_{12}H_{11-21}N$, $C_{11}H_{11-23}NO$ and $C_{15}H_{15-31}N$) and nitrogen-containing species (e.g., acetonitrile, acrylonitrile, propanenitrile, methylpentanenitrile) were specifically identified in cow dung burning emissions. Polycyclic aromatic

38   hydrocarbons (PAHs) with 9-12 carbons were identified with significantly higher abundance from coal

39   burning compared to emissions from other studied fuels. The composition of these characteristic organic

40   vapors reflects the burned fuel types and can help constrain emissions of solid fuel burning in regional

41   models.

42   **Keywords**: Vocus, solid fuel, primary emission, characteristic compounds, combustion phase

1 Introduction

44   Solid fuels (SFs), including coal and biomass, are a primary source of domestic heating worldwide (Tao

45   et al., 2018; Oberschelp et al., 2019; Wu et al., 2022). In developing regions, such as India, more than

46   80% of rural households use biomass as cooking fuel (Balakrishnan et al., 2011). Firewood is mainly

47   used for rural households, followed by crop residues and cow dung 'cakes', which are made of a mixture

48   of dried cow dung and crop residues (Loebel Roson et al., 2021; Chandramouli and General, 2011). In

49   Europe, fireplaces and woodstoves are used for domestic heating in winter, which have considerable

50   impacts on air quality, resulting in intense 'smog' events (Kalogridis et al., 2018; Fourtziou et al., 2017;

51   Bailey et al., 2019; Font et al., 2022). China is the largest producer and consumer of coal in the world.

52   In China and some Eastern European countries like Poland, coal is widely used for domestic purposes,

53   such as heating and cooking of households, due to its cost-effectiveness and easy accessibility (Guo et

54   al., 2021; Stala-Szlugaj, 2018). The combustion of these solid fuels has been recognized as the main

55   source of anthropogenic emission of atmospheric pollutants that elicit adverse effects on air quality and

56   human health (Wu et al., 2022; Zhang and Smith, 2007).

57   Wildfires or bushfires have become more frequent in many regions due to heatwaves and drought

58   (Weber and Yadav, 2020; Williams et al., 2012). SF combustion, including wildfires, is a major source

59   of non-methane organic gases (NMOGs) to the atmosphere, emitting hundreds to thousands of different

60   organic gas-phase species (Hatch et al., 2019; Koss et al., 2018; Permar et al., 2021). Once emitted,

61   evaporated vapors or freshly emitted burning NMOGs will oxidize to produce oxygenated organic gases

62   with a broad volatility range. These organic gases with sufficiently low volatility will nucleate or

63   condense onto pre-existing aerosols to form secondary organic aerosols (SOA) (Kumar et al., 2023).

64   The identification of characteristic compounds for each emission source will be highly valuable in

65   evaluating SOA formation potential and ambient source contributions. Liu et al. (2008) identified

66   potential characteristic volatile organic compounds for different emission sources (e.g., biomass

67   burning, mobile sources and painting). Nevertheless, these commonly used characteristic compounds

68   are well-established, yet due to their presence in more than one type of biomass fuel, distinguishing

69   between different biomass-burning sources presents challenges. Since 2009, there have been many

70   advancements in the gas-phase measurements of SF, which include lab studies (Bruns et al., 2017;

71   Bruns et al., 2016; Bhattu et al., 2019) and large field campaigns (e.g., WE-CAN Aircraft Measurements,

72   FIREX-AQ campaign) (Permar et al., 2021; Jin et al., 2023; Majluf et al., 2022). However, efforts

73   toward understanding SOA formation in burning plumes have been hindered by limited identification

74   and quantification of NMOGs emitted by fires, especially intermediate volatility organic compounds

75   (IVOCs) (Akagi et al., 2011). Laboratory and field campaigns suggest that intermediate volatility

76   organic compounds are important precursors of SOA. Grieshop et al. (2009) demonstrated that

77   traditional SOA precursors account for less than 20% of the observed SOA formed from residential

78   wood combustion emissions, while IVOCs can contribute approximately 70% of the formed SOA (Li
79   et al., 2024), which highlights the urgent need for more research on IVOCs from biomass burning
80   emissions.

81   Adding an IVOC emission inventory to an air quality model can significantly narrow the gap between
82   the estimated and measured SOA concentrations(Li et al., 2024; Hodzic et al., 2010; Zhao et al., 2016;
83   Robinson et al., 2007).

84   Offline sampling methods such as canisters and adsorption-thermal desorption (ATD) cartridges, along
85   with gas chromatography (GC) analysis, have limitations related to their low time resolution,
86   susceptibility to sampling artifacts, and a limited range of measurable compounds (Hatch et al., 2018;
87   Hatch et al., 2017). In addition to offline techniques, proton-transfer-reaction mass spectrometry (PTR-
88   MS) has been widely used for the online measurement of volatile organic compounds (VOCs) in the
89   atmosphere (Yuan et al., 2017). However, IVOCs still suffer from high losses in the sampling lines and
90   PTR-MS drift tubes. Furthermore, most studies have focused on either primary or aged emissions, with
91   very few examining the real-time influence of combustion conditions on the composition of emitted
92   organic gases (Bruns et al., 2016; Akherati et al., 2020; Tkacik et al., 2017). The recently developed
93   Vocus PTR time-of-flight mass spectrometer (hereafter Vocus) has greatly enhanced sensitivity due to
94   a newly designed chemical ionization source (Krechmer et al., 2018), and it can detect a broader
95   spectrum of VOCs, IVOCs, and their oxygenated products (up to six to eight oxygen atoms for
96   monoterpene oxidation products) (Li et al., 2020; Wang et al., 2021; Riva et al., 2019). With a novel
97   design and chemical ionization source, the Vocus PTR-TOF allows for real-time characterization of
98   gas-phase emissions during various burning phases (e.g., flaming and non-flaming phases) and
99   identifies the characteristic compounds for a wide range of fuels.

100   The present study compares real-time emissions from different combustion fuels. We systematically
101   characterize the primary organic gas composition using Vocus from a variety of burning fuels from
102   both residential stoves (beech logs, pine and spruce logs, and coal) and open combustion (spruce and
103   pine branches and needles, straw, cow dung). We investigate the characteristics of compounds and
104   emission factors for different combustibles and explore the dependence of individual NMOGs emission
105   intensity, variability, and chemical composition on combustion conditions (open or stove) and
106   combustion phases. We also discuss characteristic compounds for the burning fuels examined in this
107   study. The differences in EFs and profiles between different combustibles can be considerable, and
108   these results illustrate the importance of considering these emission sources individually. Measurements
109   capable of identifying and quantifying rarely measured and presently unidentified emissions of NMOGs,
110   particularly chemically complex low volatility fraction, are vital for advancing the current
111   understanding of the impact of solid fuel combustion on air quality and climate.

2 Materials and methods

2.1 Fuel and burning setup

114   The experiments were conducted at the Paul Scherrer Institute (PSI) in Villigen, Switzerland and the
115   burning facility that is part of the PSI Atmospheric Chemistry Simulation Chambers (PACS). Real-time
116   characterization of the primary gas and particle phase emissions was carried out during 28 test burns.
117   Six fuels were studied (beech, spruce, pine, straw, cow dung, and coal briquettes) with three to six

118 replicate burns. Material in the beech, spruce, and pine fuels (e.g., logs and needles) was sourced from
119 a local forestry company in Würenlingen, Switzerland. Cow dung cakes (a mixture of cow dung and
120 straw) were collected from Goyla Dairy in Delhi, India. Coal briquettes were purchased from Gansu,
121 China (Ni et al., 2021; Klein et al., 2018). These fuels are classified into four categories, representing
122 different types of burning scenarios in real life: 1) residential wood burning, 2) agricultural burning, 3)
123 forest fires, and 4) traditional heating and cooking in two regions. Residential wood burning included
124 beech and spruce/pine logs burned separately in a stove, consistent with the materials used in two
125 previous articles (Bertrand et al., 2017; Bhattu et al., 2019). Combustion of agricultural waste, straw,
126 and a mixture of fresh spruce and pine branches and needles were in an open stainless-steel cylinder
127 measuring 65 cm in diameter and 35 cm in height. Forest fires were simulated by burning a mixture of
128 spruce and pine branches and needles. Traditional cooking and heating practices in regions like India
129 are represented by burning cow dung cakes using half-open stoves (Loebel Roson et al., 2021).
130 Traditional cooking and heating practices in rural regions of developing countries are represented by
131 burning coal in a portable cast iron stove purchased from the local market (Liu et al., 2017).

132 **2.2 Instrumentation and sampling**

133 The experimental design is shown in Figure S1. In summary, it is made up of a burner and a set of
134 diluters with heated lines. Before each burn, a continuous stream of pure air was passed through the gas
135 lines overnight to avoid cross-contamination between burns and to ensure a low background of VOCs.
136 From the various combustibles, once a burn is initiated, emissions are sampled from the chimney
137 through a heated line (473 K) and diluted by two dekati diluters by a factor of ~ 100 (473 K, DI-1000,
138 Dekati Ltd.). Note that wood-burning combustion cycles consist of a first cycle referred to as the 'first
139 load' and subsequent cycles, referred to as 'reloads'. The first load consisted of a cold start, flaming,
140 smoldering, and burn-out phase, and the reloads were comprised of a warm start, flaming, smoldering,
141 and burn-out phase. NMOG emissions of solid fuel combustion are released within 10−30 min after
142 loading. We define the time until full ignition duration for burning encompasses 80% of the entire
143 process, starting from loading the fuels to burnout.

144 Numerous instruments were connected after the second dekati diluter for the characterization of both
145 the particulate and gaseous phases. A Scanning Mobility Particle Sizer (SMPS, CPC 3022, TSI, and
146 custom-built DMA) provided particle number size distribution information. The non-refractory particle
147 composition was monitored by a high-resolution time-of-flight aerosol mass spectrometer (HR-ToF-
148 AMS, Aerodyne Research Inc.). AMS data were processed using SQUIRREL (SeQUential Igor data
149 RetRiEvaL v. 1.63; D. Sueper, University of Colorado, Boulder, CO, USA) and PIKA (Peak Integration
150 and Key Analysis v. 1.23) to obtain mass spectra of identified ions in the m/z range of 12 to 120. Black
151 carbon was measured with an Aethalometer (Magee Scientific Aethalometer model AE33) (Drinovec
152 et al., 2015) with a time resolution of 1 minute. A LI-7000 CO_2 analyzer (LI-COR) provided continuous
153 measurements of carbon dioxide (CO_2). The concentrations of total hydrocarbons (THC) and methane
154 (CH_4) were monitored using a flame ionization detector monitor (THC monitor Horiba APHA-370).

155 We deployed a Vocus to measure organic vapors with a wider range of volatilities. A detailed
156 description of the Vocus is provided elsewhere (Huang et al., 2021; Krechmer et al., 2018). For this
157 study, the Vocus was operated with H_3O^+ as the reagent ion. The sample air was drawn in through a 1
158 m long polytetrafluoroethylene (PTFE) tube (6 mm o.d.) using a total sample flow of 4.3 L/min, which

159 helped reduce the losses in the inlet wall and the sampling delay. Of the total sample flow, only 100-
160 150 cm³/min went to Vocus, and the rest was exhausted. The Vocus was calibrated before and after
161 measurements every day using a multi-component standard cylinder (Tofwerk AG). Standard gases
162 were diluted by the injection of zero air, producing mixing ratios of VOCs of around 20 ppbv. The
163 calibration components were methanol, acetaldehyde, acetonitrile, acetone, acrylonitrile, isoprene,
164 methyl ethyl ketone, benzene, toluene, m-xylene, α-pinene and 1,2,4-trimethylbenzene. The
165 background measurements were performed using dry zero air every day. Data were recorded with a
166 time resolution of 1 s. The raw data were processed using Tofware v3.2.3 software (TOFWERK,
167 Aerodyne, Inc.). The standard non-targeted analysis workflow developed by Tofwerk was adopted for
168 mass calibration and peak fitting. The mass transmission function and the ratios between the measured
169 and calculated sensitivities for a series of ions were used to quantify the data and convert the ion counts
170 to ppbv. To calculate the mixing ratio for compounds not present in the calibration mixture, the slope
171 of the linear fit was multiplied by the proton transfer rate constants (k_{ptr}) which have been provided in
172 Supplement Table.

173 **2.3 Data analysis**

174 Modified combustion efficiency (MCE, Equation 1) is an estimate of the relative amount of flaming
175 and smoldering and is equal to

$$MCE = \frac{\Delta CO_2}{\Delta CO + \Delta CO_2}$$

Equation (1)

176 Where ΔCO, ΔCO_2 are the excess mixing ratios of CO or CO_2, respectively (Ward and Radke, 1993).
177 Generally, a higher MCE (> 0.9) suggests dominated flaming combustion, whereas a lower MCE (<
178 0.9) is mostly associated with smoldering combustion (Zhao et al., 2021; Zhang et al., 2022).

179 Primary emission factors (EFs, g kg⁻¹) of conventional gases (CO_2, CO, and CH_4), NMOGs (Vocus)
180 and particle phase species were calculated, following a carbon-mass balance approach (Andreae and
181 Merlet, 2001)

$$EF_i = \frac{m_i}{\Delta CO + \Delta CO_2 + \Delta CH_4 + \Delta NMOGs + \Delta OC + \Delta BC} \times \cdot W_C$$

Equation (2)

182 Here m_i refers to the mass concentration of species i. ΔCO, ΔCO_2, ΔCH_4, $\Delta NMOGs$, ΔOC, and ΔBC
183 are the background-corrected carbon mass concentrations of carbon-containing species in the flue gas.
184 OC is derived from the OM / OC ratio determined with high-resolution AMS analysis (Canagaratna et
185 al., 2015). W_C is the carbon mass fraction of the burning fuel. The W_C in the fuel a constant average
186 value of 0.46 for wood (Bertrand et al., 2017), 0.45 for straw (Li et al., 2007), 0.45 for cow dung (Font-
187 Palma, 2019), and 0.49 for coal (Zhang et al., 2000) was assumed. Changes of W_C over the burning
188 cycle are expected to be small compared to the variability of pollutant emissions.

189 **2.4 Volatility calculation of gaseous organic compounds**

190 The volatility (i.e. the saturation mass concentration, C*) for individual organic compounds was
191 calculated based on the number of oxygen, carbon, and nitrogen atoms in the compound using the
192 approach by Li et al. (2016):

193
$$log_{10}{}_C^* = \left(n_C^0 - n_C^i\right)b_C - n_O^i b_O - 2\frac{n_C^i n_O^i}{n_C^i + n_O^i}b_{CO} - n_N^i b_N$$
Equation (*3*)

194 where n_C^0 is the reference carbon number; n_C^i, n_O^i and n_N^i denote the numbers of carbon, oxygen, and

195 nitrogen, respectively, in the compound. b_C, b_O and b_N are the contributions of each atom to $log_{10}{}_C^*$,

196 respectively; and b_{CO} is the carbon-oxygen nonideality. The parameters used in this analysis are

197 presented in Table S1. Most notably, the empirical approach used by Li et al. (2016) was derived with

198 only a limited number of organonitrates, which could potentially introduce bias in estimating vapor

199 pressure (Isaacman-Vanwertz and Aumont, 2021). To mitigate this bias, we modified the nitrogen

200 coefficient for CHON formulas that can be forced to equal twice the negative of the oxygen atom ($b_N =$

201 $-2b_0$).

2.5 Identification of characteristic compounds

203 In this study, the mixing ratio relative contribution for more than 1500 species from six different fuels

204 for all 28 test burns was quantified by using Vocus. To identify the characteristic compounds of

205 emissions from different fuels, we implemented the Mann-Whitney U test (Mann and Whitney, 1947;

206 Wilcoxon, 1945) in MATLAB®, which has been applied in the selection of aerosol markers (Zhang et

207 al., 2023). It is a nonparametric test and is used for between-group comparisons when the dependent

208 variable is ordinal or continuous and not assumed to follow a normal distribution.

209 This test takes two data samples as parameters, uses the ranks as a measure of central tendency, and

210 then returns the test results with a *p*-value to indicate the statistical significance. When the *p*-value is

211 lower than the significance level of 0.1 (a commonly used *p*-value to study statistical significance in

212 atmospheric research), the median of the tested sample is significantly high or low in the two-tailed test.

213 However, due to the similarity in fuel types between burning spruce and pine logs, as well as spruce

214 and pine branches and needles, they were categorized as separate fuel sources for this test and not

215 compared with each other but were only compared with the other four types of fuels. Similarly, due to

216 the composition of cow dung "cakes," which comprise a mixture of dried cow dung and crop residues

217 and a relatively high correlation between cow dung and straw (Figure 1), the Mann-Whitney U test was

218 carried out without accounting for the presence of the other fuels.

219 The molecules from a specific class of fuel that satisfy the pairwise comparison test between one fuel,

220 referred to as fuel *j*, and other types of fuel, were determined to be significantly high- or low-fraction

221 ions in fuel *j*. These ions have the potential to serve as characteristic compounds for fuel *j*. We have

222 calculated in addition the fold change (*FC*) of ion *i* in fuel *j* was calculated using Equation 4,

$$FC_{i,j} = \frac{f_{i,j}}{f_{i,other}}$$
Equation (4)

223 Where $f_{i,j}$ represents the fraction of ion *i* in the mass spectra profiles of fuel *j*, and $f_{i,other}$ represents

224 the average fraction of ion *i* in the mass spectra from the other fuels.

3 Results and discussion

3.1 Emission factors from solid-fuel combustion

The average EFs of CO, CO_2, NMOGs and PM in g/kg as well as the MCE values calculated for the 6 types of fuels, are shown in Table 1. Detailed EFs and MCE values for each experiment can be found in Table S2.

The average MCE values depend on the fuel types and combustion phases (flaming and smoldering). The lowest MCE values, 0.90, were observed during the smoldering phase of the stove-burning of beech logs, while the highest values, at 0.99 ± 0.02, were recorded during the flaming phase of the spruce and pine branches and needles open burning. In all experiments, the highest EFs for a single gas-phase species correspond to CO_2 (1136.2-1711.7 g/kg). Coal burning has the highest average CO EFs (40.6 ± 12.6 g kg^{-1}) and CO_2 EFs (1680.2 ± 32.7g kg^{-1})

Total NMOG EFs reported in Table 1 refer to species quantified using the Vocus. The average EFs of primary organic gases (in the range of 6.7 to 74.2 g kg^{-1}) and the standard deviation are calculated based on the average EFs for the repeatable experiments, which depend on the combustion phases and fuel types. Generally, lower MCE values correspond to higher NMOGs EFs within a given class of burning fuel (Figure S2a). For instance, smoldering beech logs resulted in significantly higher average NMOGs EFs (74.2 ± 42.9) compared to burning pine and spruce logs. Pine and spruce stove and open burning, dominated by the flaming phase (average MCE > 0.95), exhibited average NMOGs EFs of 44.9 ± 17.5 and 39.8 ± 11.4, respectively. The slightly higher EFs for pine and spruce wood burning can be attributed to the more extensive analysis of NMOGs in our study compared to previous research (37.3 g/kg) (Hatch et al., 2017). Despite the slight difference in MCE for some experiments, the increasing EFs for NMOGs with at least six carbon atoms per molecule ($\geqslant$ C6) as proxy SOA precursors were observed with lower MCE (Figure S2b) (Bruns et al., 2016). Moreover, the EFs of these SOA precursors are much higher than the primary biomass-burning organic aerosol (BBOA), which suggests a higher potential for SOA formation. Notably, the emission of NMOGs from cow dung and coal was relatively low, at 6.7 ± 2.1 and 11.5 ± 2.6 g kg^{-1}, respectively. Our emission factors align well with previously reported volatile organic compound emission factors from bituminous coal combustion under similar conditions (range of 1.5 to 14.1 g/kg) reported by (Klein et al., 2018).

3.2 Chemical composition of primary organic vapors

3.2.1 Overview of the measurements

To assess the feasibility of distinguishing differences between combustion fuel sources based on the measured species, we evaluated the similarity of the mass spectra obtained from each experiment using the correlation coefficient (r), as shown in Figure 1. Primary NMOGs from the same burning fuel are strongly correlated (0.82-0.99), indicating the general repeatability of the experiments. Furthermore, we observed a weak intra-fuel correlation between coal and other biomass sources (0.44-0.78), suggesting significant differences in chemical composition. By contrast, the separation between different biomass samples is not stark and all possess a correlation between 0.6-0.98. We also note the slight difference in composition between smoldering and flaming beech wood.

263   Figure 1 also shows the average mixing ratio contribution of full ignition duration from m/z 40 to 300
264   for each experiment, and is categorized into C_xH_y, $C_xH_yO_z$, C_xH_yN and $C_xH_yO_zN$ families based on their
265   elemental composition. In all primary NMOGs, the $C_xH_yO_z$ family is the most abundant group, making
266   the largest contribution to beech logs (88.6%), pine and spruces logs (82.1%) and straw (81.7%). These
267   percentages are higher than those for coal (63.1%) and cow dung (68.9%). Coal burning results in
268   considerably higher contributions in the C_xH_y families (33.7%) than beech logs (9.3%), consistent with
269   the bulk chemical composition of the fuels.

270   Figure 2 separates emitted compounds based on their carbon (x-axis) numbers. The dominant signals
271   in primary organic gases for all fuels are attributed to C3-6 compounds, while more species with higher
272   carbon numbers (#C > 10) are observed in pine and spruce branches and needles open burning. The
273   bin containing H/C ratios between 1.2 and 1.5 has the largest contribution in all fuels except the straw,
274   ranging from 27% to 31.2%. O/C ratios less than 0.15 contribute significantly to coal burning (42%),
275   which corresponds to the high proportion of C_xH_y families (Figure 1). Wood and straw burning emitted
276   more oxygenated organic vapors than coal and cow dung burning with more contribution of higher O/C
277   species (O/C> 0.5). The results show similarities to the comparison between burning wood and cow
278   dung in the particle phase. Specifically, cow dung exhibits a slightly lower fraction of high O/C
279   compared to other fuels studied. (Zhang et al., 2023).

280   Generally, the total fraction of nitrogen-containing species (C_xH_yN and $C_xH_yO_zN$) is significantly higher
281   in the primary NMOGs emitted from open burning of cow dung (18.8%) compared to the other fuels
282   (2.1% to 7.3%). This trend is consistent with both our results from aerosol composition measurement
283   and previous literature (Stewart et al., 2021b; Zhang et al., 2023; Loebel Roson et al., 2021). Generally,
284   nitrogen containing compounds in cow dung consist mainly of one nitrogen atom and have a wide range
285   of carbon numbers between 2 and 7 (Figure 2). Stewart et al. (2021a) also reported that cow dung was
286   the largest emitter of nitrogen-containing NMOGs than other fuelwood and crops in India, releasing
287   large amounts of acetonitrile and nitriles. These nitrogen-containing organic gases are likely formed
288   from the volatilization and decomposition of nitrogen-containing compounds within the cow dung cake,
289   such as free amino acids, pyrroline, pyridine, and chlorophyll (Ren and Zhao, 2015; Burling et al., 2010).

290   We categorized NMOGs by functional groups into 10 classes, including alcohols, carbonyls (including
291   acid), hydrocarbons, furans, N-containing compounds, O-containing < 6 (where the number of carbon
292   atoms is less than 6), O-containing ≥ 6 (where the number of carbon atoms is equal or greater than 6),
293   oxygenated aromatics, polycyclic aromatic hydrocarbons (PAHs), single-ring aromatics (SRA) (Bhattu
294   et al., 2019). Figure S3 and Figure S4 show a comparison of the organic gas composition observed from
295   different fuel types. The measured emissions exhibit significantly different compositions, reflecting the
296   variability of organic components produced from different fuel types. The emissions of all solid fuels
297   are overwhelmingly dominated by carbonyls in the range of 23.1% (coal) to 45.1% (straw). For all
298   emissions, furans represent the second largest group, which account for more than 14% of the emissions.
299   Comparatively, aromatic compounds are less significant in biomass burning: 5.9% - 12% for
300   oxygenated aromatics, 0.5% - 2.1% for PAHs, and 2.1% - 5.8% for SRA. In contrast, aromatic
301   emissions are relatively larger in coal burning emissions (13.6%, 8.1%, and 13.8%, respectively).

3.2.2 Volatility of organic compounds

302

303 Based on the $\log_{10}C^*$ values of all organic compounds parameterized with the modified approach of Li
304 et al. (2016) described in Sect. 2.4, the gaseous organic compounds were grouped into a 14-bin volatility
305 basis set (Donahue et al., 2006) (Figure 3). We choose to classify the volatility in four main classes with
306 units of µg m^{-3}: VOCs as $\log_{10}(C^*) > 6.5$, IVOCs as $\log_{10}(C^*)$ between 6.5 to 2.5, semi-VOCs (SVOCs)
307 as $\log_{10}(C^*)$ between 2.5 to - 0.5 and low-VOCs (LVOCs) as $\log_{10}(C^*) < - 0.5$).

308 Comparison and compilation of gaseous biomass burning emissions sorted by volatility and functional
309 group are shown in Figure 3, and the distribution of average EFs as a function of binned saturation
310 vapor concentration is shown. The VOC class was found to be the most abundant, ranging from 58.7%
311 to 87% (Figure S5). For all burns, carbonyls, furans, and SRA families are overwhelmingly dominant
312 in VOCs, accounting for more than 60% of the VOC emissions. The high fraction of oxygenated VOCs
313 like carbonyls in biomass burning emissions is in stark contrast to VOCs emitted from coal combustion,
314 which is dominated by aromatic hydrocarbon emissions, particularly PAHs. This difference may be
315 attributed to the condensed structure of coal. PAHs are a group of organic matter compounds containing
316 multiple aromatic rings that mainly result from incomplete combustion (Mastral and Callen, 2000).

317 IVOCs also constituted a considerable fraction in solid-fuel combustions (from 12.6% to 39.3%),
318 particularly in spruce and pine branches and needles (39.3%), cow dung (24.3%) and coal (31.1%)
319 (Figure S5). Significant differences in the bulk volatility of organic compounds were observed among
320 different types of wood burning. In general, spruce and pine branches and needles open burning released
321 a higher proportion of IVOCs (39.3%) into the gas phase compared to stove logs burning (12.6% and
322 23.9%). Pallozzi et al. (2018) also reported a similar result, showing that needle/leaf combustion
323 released a greater amount of volatile organic compounds into the atmosphere than branch combustion.
324 This difference may be attributed to a lower percentage of terpenes in woody tissues compared to
325 needle/leaf tissues (Greenberg et al., 2006). In addition, open burning provides more oxygen than stove
326 burning, which enhances the formation of partially oxidized organic compounds. Within the open
327 burning experiments, the oxygenated molecules (both aromatics and C ≥ 6) are enhanced relative to the
328 other experiments and result in the largest emission factors of IVOCs. In addition to the burning
329 conditions, the fuel properties are also an important factor affecting the IVOC component. Notably,
330 cow dung comprised a higher fraction of N-containing species within their IVOC emissions compared
331 to other fuels. The emission in volatility bins in this study is important for the modeling of organics
332 with the VBS scheme.

3.3 Comparison between flaming and smoldering of wood burning

333

334 Figure 4a shows a typical burning cycle during beech log wood experiments with distinct emission
335 characteristics between flaming and smoldering phases. In the top panel, the MCE is used to indicate
336 the flaming stage with a significant CO_2 enhancement, while the smoldering stage exhibits high levels
337 of CO. The flaming phase shows considerable BC emission, while the smoldering phase is dominated
338 by OA emissions without visible flame. The AAE during the smoldering phase is approximately twice
339 that of the flaming phase, possibly due to the presence of "brown carbon" in organic aerosols. *f*60
340 represents the prevalence of primary combustion products such as levoglucosan and is used as an
341 indicator for fresh BB emissions (Schneider et al., 2006; Alfarra et al., 2007). During the
342 starting/flaming phase, when the temperature is higher, *f*60 increases, whereas for lower temperatures

343 in the smoldering phase, f60 decreases (Weimer et al., 2008). The mixing ratio of most of the
344 compounds correlates negatively with the MCE as expected with a significant increase in the
345 smoldering phase (Figure 4a and Figure S6). However, some compounds like benzene have different
346 enhancement rates from flaming to smoldering, which is similar to previous studies (Warneke et al.,
347 2011).

348 Figure 4b illustrates the measured emission factors for flaming and smoldering wood fire stages. On
349 average, emission factors for organic gases in the flaming stage are approximately four times lower
350 (31.4 g/kg) than those in the smoldering stage fires (121.9 g/kg). Despite significant variability in
351 organic gas emission strengths, the relative contribution of different classes showed large similarities
352 among combustion phases (Figure S7). Hardwood (beech) is a fibrous substance primarily composed
353 of three chemical elements: carbon, hydrogen, and oxygen and these basic elements are incorporated
354 into several organic compounds, i.e. cellulose, hemicellulose, lignin, and extractives formed into a
355 cellular structure (Asif, 2009). The flaming stage is associated with more complete oxidation with a
356 relatively higher contribution of OVOCs (e.g., furan, oxygenated aromatics, O-containing, Figure S8).
357 Conversely, during the smoldering stage, more CO and organic gases are emitted relative to the flaming
358 stage (Figure 4a). OVOCs, such as carbonyl, furan, oxygenated aromatics, and O-containing species,
359 form the major fraction (> 88%) of emissions in both flaming and smoldering fires. They are followed
360 by the sum of C_xH_y, and SRA (5-10%). As shown in Figure S9, the volatility distribution of beech log
361 stove burning between the flaming phase and smoldering phase is also similar, only with a relatively
362 higher contribution of carbonyls and C_xH_y in the smoldering phase than flaming phase. This suggests
363 that the emission factor plays a more important role than the chemical composition in differentiating
364 between flaming and smoldering fires.

3.4 Common compounds emission for biomass-burning combustion and identification of
characteristic compounds for different fuels

3.4.1 Common compounds for biomass burning

368 To conduct a comprehensive analysis aimed at identifying characteristic compounds among emissions,
369 the Mann-Whitney U test (refer to Sect. 2.5) was performed on the relative contribution of primary
370 organic gases derived from various fuels as measured by Vocus. The results of the pairwise Mann-
371 Whitney test are presented in Figure S10, illustrating the average $-\log_{10}$ of the p-value as a function of
372 the $\log_2$ of the fold change (FC). Species that yield p-values lower than 0.1 in the two-tailed test for all
373 pairwise comparisons are deemed significantly more abundant or scarce in a particular fuel type
374 compared to all other fuels. These species are indicated as colored circles in Figure 5. In cases where
375 species do not meet this criterion once or multiple times, they are represented as gray circles, even if
376 their average p-value falls below 0.1. A higher $-\log_{10}(p$-value) signifies a reduced likelihood that the
377 fractional medians of two species are equivalent. Simultaneously, a greater FC (as per Equation 4)
378 indicates an increased presence of the species' fractional contribution in the tested fuel in comparison
379 to the average contribution across all other fuels. This suggests a higher degree of exclusivity for this
380 species in the given context. The selected characteristic compounds, p-values, fold changes, and
381 threshold results are listed in the Supplement Table.

382 As shown in Figure 1, biomass fuels (wood, straw and cow dung) are different fuels from coal in this
383 study. To address this, we characterized the common compounds from varied biomass fuels by

384   establishing a threshold (relative mixing ratio contribution $\geqslant 0.1\%$) for compounds that are not specific

385   characteristic compounds of biomass burning, which allowed for the identification of compounds that

386   are more readily detectable in intricate environments. As shown in Figure S11, the gas-phase analysis

387   revealed several dominant species: $C_5H_4O_2$ (furfural, 2.2-10.1%), $C_2H_4O_2$ (acetic acid, 2.1-5.8%),

388     $C_3H_6O_2$ (methyl acetate, 1.7-4.6%), and C_2H_4O (acetaldehyde, 1.3-3.9%), which were also reported

389   prior studies on biomass burning (Bruns et al., 2017; Stockwell et al., 2015; Christian, 2004; Sarkar et

390   al., 2016). Furthermore, the category of common compounds represents the primary set of compounds

391   associated with biomass burning, contributing from 46% to 69% of the emissions (Figure S12). Carter

392   et al. (2022) expand the representation of fire NMOGs in a global chemical transport model, GEOS-

393   Chem, which contributes substantially to atmospheric reactivity, both locally and globally. Our results

394   could provide more input information for global or regional chemistry transport models.

3.4.2 Characteristic compounds for solid-fuel combustion

396   Mass defect plots of characteristic compounds are visualized in Figure 5, for each burning source,

397   respectively. Many characteristic compounds are identified for each unique type of burning

398   (Supplement Table). As shown in Figure 5, characteristic compounds of all wood burning are mainly

399   composed of compounds from the C_xH_y and $C_xH_yO_z$-family. However, the selected characteristic

400   compounds for spruce and pine branches and needles have higher molecular weights and are more

401   oxidized, which aligns with their characteristics of the mass spectrum. In contrast, compounds from

402   open burning of straw and cow dung contribute considerably more to nitrogen-containing families but

403   less to oxygen-containing species, consistent with their bulk chemical composition characteristics.

404   Additionally, characteristic compounds for coal consist mainly of compounds from C_xH_y-family, which

405   also aligns with its bulk chemical composition and relatively higher H/C ratios (Figure 2).

406   For all softwood (i.e., spruce and pine logs and spruce and pine branches and needles in this study),

407   monoterpenes ($C_{10}H_{16}$) are a characteristic compound along with the fragment at m/z 81.07 (C_6H_8).

408   However, monoterpenes cannot exclusively be related to biomass burning given their abundance in the

409   atmosphere. Monoterpenes are also the biogenic volatile organic compounds (BVOCs) emitted from

410   natural trees and other vegetation (Hellén et al., 2012). However, the emission rates of terpenes vary

411   with season, with a higher rate in spring and summer and a lower rate in autumn and winter (He et al.,

412   2000; Noe et al., 2012). In winter, monoterpenes could be a characteristic compound for softwood

413   burning due to minor natural emissions from spruce, but in summer, terpene emissions from natural

414   trees would dominate the contribution making it a non-characteristic compound. P-cumenol ($C_9H_{12}O$),

415   as one of the characteristic compounds for beech logs, was discovered to be one of the prominent

416   products of beech wood pyrolysis of lignins (Sengpiel et al., 2019; Keller et al., 2020). Homologues of

417     $C_{10}H_{8-18}O_2$ are determined for spruce and pine branches and needles, with $C_{10}H_{10}O_2$ being β-

418   phenylacrylic acid, which is one of the main chemical compositions of the extract of the cedar pine

419   needle. $C_{10}H_{14}O_2$ could be 1-guaiacylpropane, which is proposed as a characteristic compound for

420   coniferyl-type lignin pyrolysis products from pine (Simoneit et al., 1993; Liu et al., 2021). Homologues

421   of $C_{11}H_{8-18}O_2$ are also seen, for example, $C_{11}H_{14}O_2$, likely 1-(3,4-dimethoxy-phenyl)-1-propene, which

422   is stated as a representative compound found in lignin (Alves et al., 2003; Hill Bembenic, 2011).

423   Noticeably, cow dung has a significantly different chemical composition. As a result, many

424   characteristic compounds are identified from the burning of cow dung compared to other fuels. These

425 characteristic compounds predominantly contain nitrogen in chemical composition and overlap all
426 characteristic compounds for straw, owing to the mixture of dried cow dung and crop residues in "cow
427 dung cakes." Many nitrogen-containing characteristic compounds are found in straw and cow dung,
428 such as C_4H_5N, C_5H_5N, C_5H_7N, and C_6H_7N, which could likely be assigned to pyrrole, pyridine,
429 methylpyrrole and methyl pyridines respectively. Pyrolysis of the constituents in the crop residue is a
430 probable pathway for these compounds (Ma and Hays, 2008). Acetonitrile (C_2H_3N), acrylonitrile
431 (C_3H_3N), propanenitrile (C_3H_5NO), and 4-methylpentanenitrile ($C_6H_{11}N$) were found as characteristics
432 compounds for cow dung with generally higher FC and higher relative contribution. Additionally,
433 several series of nitrogen-containing homologues are found, such as $C_{10}H_{11-21}NO$, $C_{12}H_{11-21}N$, $C_{11}H_{11-23}NO$
434 $_{23}NO$ and $C_{15}H_{15-31}N$. These nitrogen-containing gases have also been detected, especially in emissions
435 from cow dung cake in India compared to fuelwood and are likely formed from the volatilization and
436 decomposition of nitrogen-containing compounds within the cow dung cake. These compounds
437 originate primarily from free amino acids but can also arise from pyrroline, pyridine, and chlorophyll
438 (Stewart et al., 2021a).

439 Coal is also a distinct solid fuel compared to other biomass fuels in this study, showing a relatively
440 lower correlation coefficient (Figure 1). Consequently, many series of C_xH_y-family homologues are
441 found. Compounds with 9-12 carbon atoms, as shown in Figure 5 for coal burning, could be PAHs-
442 related, such as C_9H_8 (1-Indene), $C_{10}H_8$ (naphthalene), $C_{10}H_{10}$ (1-methylnapthalene), $C_{12}H_{10}$
443 (acenaphthene), $C_{12}H_{12}$ (2,6-dimethylnaphthalene). The EFs of the characteristic compounds also show
444 an increasing trend with the decrease of MCE (Figure S13), which suggests EFs of the characteristic
445 compounds are not only dependent upon the type of fuel burnt but also on the burning condition.

4 Conclusions

447 In this study, we first investigated the real-time emissions of primary organic gases using Vocus-PTR-
448 TOF during typical solid fuel combustion, including residential burning (beech logs, a mixture of spruce
449 and pine logs, and coal briquettes) and open combustion (spruce and pine branches and needles, straw,
450 and cow dung). Average emission factors of CO, CO_2, primary organic gases and PM were calculated.
451 This work provides a comprehensive laboratory-based analysis of the chemical composition of organic
452 gases emitted from the different combustibles and different combustion phases. We discuss the
453 prominent net combustion emissions from biomass burning and identify new characteristic compounds
454 using the Mann-Whitney U test.

455 The results indicate that wood burning has higher primary organic gas emission factors compared to
456 other fuels. The emissions varied significantly, ranging from 6.7 to 74.2 g kg^{-1}, depending on the
457 combustion phases and fuel types. Despite the slight difference in modified combustion efficiency
458 (MCE) for some experiments, the increasing EFs for primary organic gases were observed with lower
459 MCE. Moreover, the EFs of these SOA precursors are much higher than the primary biomass-burning
460 organic aerosol (BBOA), which suggests a higher potential for SOA formation. The $C_xH_yO_z$-family is
461 the most abundant group (63.1% to 88.6%) for all solid fuels, followed by C_xH_y (9.3% to 33.7%). A
462 larger contribution of nitrogen-containing species (C_xH_yN and $C_xH_yO_zN$) is found in cow dung burning,
463 while coal burning has a higher contribution from the C_xH_y families. Moreover, the VOC class was
464 found to be the most abundant (58.7% to 87%), followed by the IVOC class (12.6% to 39.3%). Primary
465 semivolatile/intermediate-volatility organic compounds (S/IVOCs) have been proposed as important

466   SOA precursors from biomass burning. Li et al. (2024) found that IVOCs from residential wood burning
467   (~ 13% of total organic gases) can contribute ~70% of the formed SOA. Overall, these data will help
468   update the IVOC emission inventory and improve the estimates of SOA production. Specifically, these
469   results demonstrate that open burning (e.g., wildfire) emissions have enhanced IVOC emission factors,
470   suggesting that the SOA potential from open-burning sources is larger in comparison to their wood
471   stove counterparts.

472   Distinct particulate/gas emissions at different combustion phases are observed for stove burning of
473   beech logs: initial compositions of flaming or smoldering plumes were dominated by BC or OA,
474   respectively, with much higher primary organic gas emission in smoldering. Despite the large
475   variability in organic gas emission strengths, the relative contribution of different classes showed large
476   similarities among combustion phases. Therefore, the enhanced emission factor under smoldering
477   conditions means there is a greater potential for SOA formation when compared to flaming conditions.

478   However, each source generally emits a wide spectrum of organic gas species, leading to considerable
479   overlap between organic gas species from different sources. Based on the Mann-Whitney U, we selected
480   species that were unique in certain emissions as possible characteristics compounds for the
481   characteristic compounds and the common compounds for all biomass fuels. Due to minor natural
482   emissions from spruce in summer, monoterpene ($C_{10}H_{16}$) and its fragment could be characteristic
483   compounds for all softwoods (i.e., pine logs and spruce and pine branches and needles in this study) in
484   winter. More products of the pyrolysis of coniferyl-type lignin and the cedar pine needle extract could
485   be found in spruce and pine branches and needles open burning (e.g., $C_{10}H_{14}O_2$, $C_{11}H_{14}O_2$, $C_{10}H_{10}O_2$).
486   The prominent product ($C_9H_{12}O$) resulting from the pyrolysis of beech lignin is identified as the
487   characteristic compound for beech log stove burning. Many series of nitrogen-containing homologues
488   and nitrogen-containing species (e.g., acetonitrile, acrylonitrile, propanenitrile, methylpentanenitrile)
489   are identified (e.g., $C_{10}H_{11-21}NO$, $C_{12}H_{11-21}N$, $C_{11}H_{11-23}NO$ and $C_{15}H_{15-31}N$), particularly from open
490   burning of cow dung. Coal is a unique solid fuel compared to biomass and more PAHs-related
491   characteristic compounds are identified from coal burning with 9-12 carbon. These characteristic
492   compounds provide important support for future global or regional chemistry transport modeling and
493   source apportionment. Overall, our study provides a comprehensive understanding of the molecular
494   composition and volatility of primary organic compounds, as well as new insights into the identification
495   of characteristic compounds from the burning of solid fuels.

496

497

498

499

500

501

Tables and figures

Table 1 Average emission factors of CO, CO_2, Organic gases and PM as well as MCE for 6 types of burning.

Burning type	Carbon content	MCE	Emission factors (g kg^{-1} fuel)			
			CO	CO_2	NMOGs	PM
beech logs stove (n=6)	0.46	0.96 ± 0.03	38.9 ± 25.9	1409.4 ± 177.1	74.2 ± 42.9	2.5 ± 1.7
spruce and pine logs stove (n=5)	0.46	0.97 ± 0.01	28.5 ± 14.3	1511.7 ± 68.5	44.9 ± 17.5	1 ± 0.6
spruce and pine branches and needles open (n=3)	0.46	0.99 ± 0.001	2.8 ± 0.8	1579.2 ± 29.7	39.8 ± 11.4	0.9 ± 0.4
straw open (n=4)	0.45	0.97 ± 0.01	24.4 ± 6.6	1488.4 ± 87.2	42.6 ± 33.7	2.8 ± 0.7
cow dung open (n=5)	0.45	0.98 ± 0.01	21.6 ± 14.5	1583.8 ± 37.8	6.7 ± 2.1	1.6 ± 1
coal stove (n=5)	0.49	0.96 ± 0.01	40.6 ± 12.6	1680.2 ± 32.7	11.5 ± 2.6	0.9 ± 0.3

504
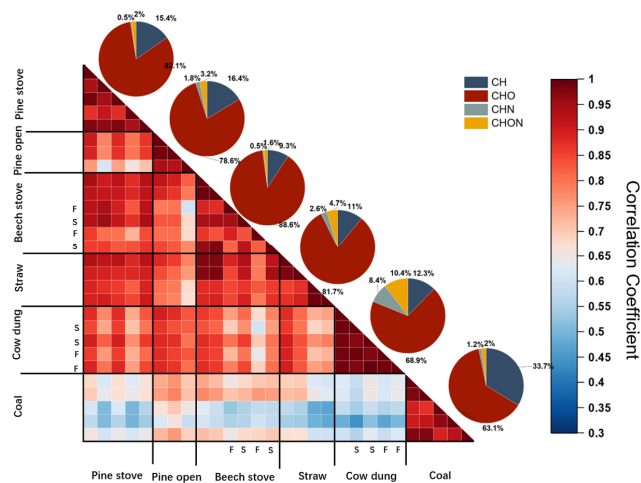
Figure 1. The correlation matrix of primary organic gases measured with Vocus (F represents flaming phase and S represents smoldering phase and unmarked columns and rows represent mixtures of both flaming and smoldering phases). Pie charts showing the contribution of elemental families are on the diagonal.

508
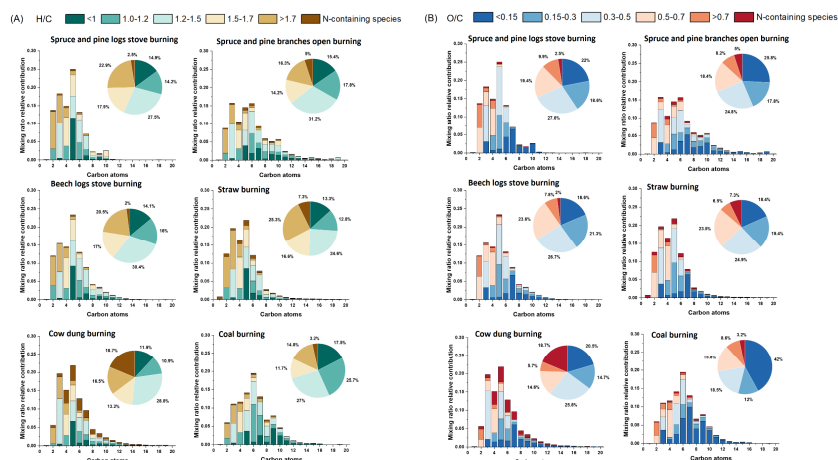
Figure 2. The average carbon distribution is colored by the H/C (**A**) and O/C (**B**) for non-N-containing species. The pie charts are the corresponding contribution of a range of H/C or O/C ratios.
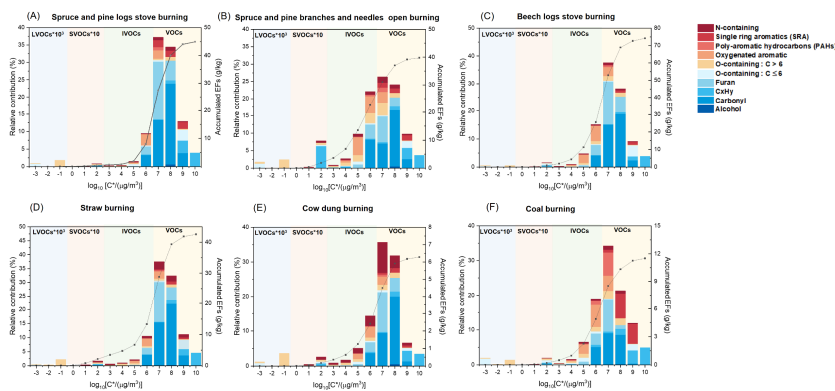
Figure 3. Volatility and average accumulated emission factors (assume the average molecular weight of each bin are same) the distribution of primary emissions as a function of binned saturation vapor concentration. Shaded areas indicate the volatility ranges with units of µg m^{-3}: VOCs (yellow) as $\log_{10}(C^*) > 6.5$, IVOCs (blue) as $\log_{10}(C^*)$ between 6.5 to 2.5, semi-VOCs (SVOCs, green) as $\log_{10}(C^*)$ between 2.5 to - 0.5 and low-VOCs (LVOCs, orange) as $\log_{10}(C^*) < - 0.5$. The relative contribution of LVOCs and SVOCs are multiplied by a factor of 1000 and 10, respectively.
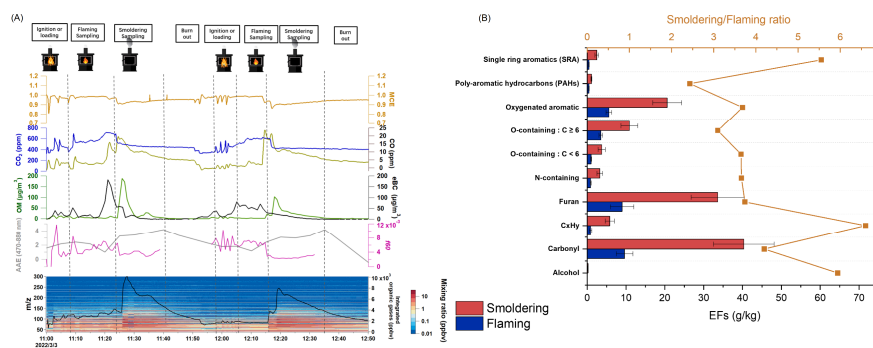
520 **Figure 4.** (A) Temporal profiles of mixing ratios measured by Vocus and evolution of CO, CO_2, AAE, f60, MCE
521 and key aerosol compositions during burning cycles of beech logs stove burning (B) Geometric mean of the
522 primary emission factors for gas-phase species of different functional groups during flaming and smoldering phase,
523 respectively (the flaming and smoldering was separated by the experimental record and calculated MCE). Error
524 bars correspond to the sample geometric standard deviation of the replicates. The square represents the mixing
525 ratio between smoldering and flaming. In this study, the MCE is used to indicate the flaming stage and smoldering
526 and a significant decrease of MAC and CO_2 was observed from the flaming phase to the smoldering phase.
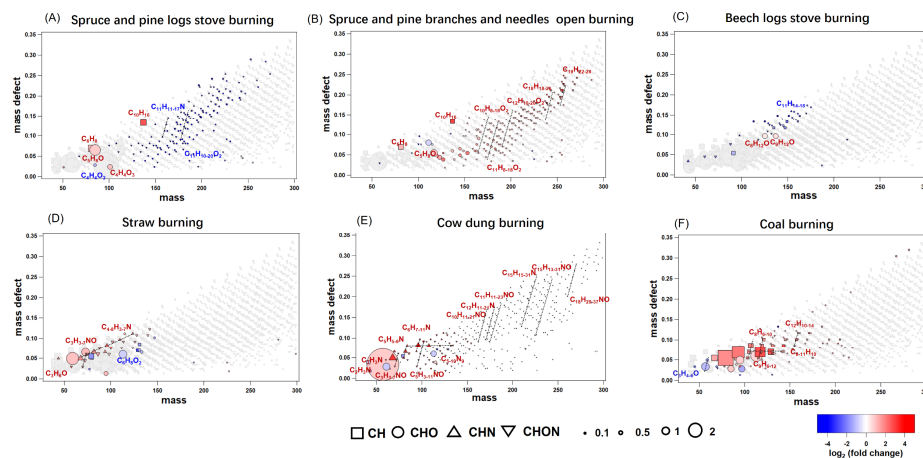
Figure 5. Mass defect plots identifying characteristic compounds sized by the square root of fractional contribution (%) and colored by $\log_2$ (the fold change). The dashed line represents the series of homologues.

Data availability

The data presented in the text and figures are available in the Zenodo online repository (https://doi.org/10.5281/zenodo.10804011).

Author contributions

TTW, JZ, HL, KL, RKYC, EG, LK, DMB, and RLM conducted the burning experiments. TTW analyzed the data and wrote the paper. MB, ZCJD, LK, DMB, KL, RLM, IEH, HL, JGS, and ASHP participated in the interpretation of data.

Competing interests

The authors declare that they have no conflict of interest.

Acknowledgments

This work was supported by the Swiss National Science Foundation (SNSF) SNF grant MOLORG (200020_188624), an SNSF Joint Research Project (grant no. IZLCZ0_189883), the PSI career return fellowship, and the European Union's Horizon 2020 research, innovation programme under the Marie Skłodowska-Curie grant agreement No 884104 (PSI-FELLOW-III-3i) and ATMO-ACCESS. PSI's atmospheric simulation chamber is a facility of the ACTRIS ERIC and receives funding from the Swiss State Secretariat for Education, Research and Innovation (SERI grant).

Reference

Akagi, S., Yokelson, R. J., Wiedinmyer, C., Alvarado, M., Reid, J., Karl, T., Crounse, J., and Wennberg, P.: Emission factors for open and domestic biomass burning for use in atmospheric models, Atmos. Chem. Phys., 11, 4039-4072, 2011.

550 Akherati, A., He, Y., Coggon, M. M., Koss, A. R., Hodshire, A. L., Sekimoto, K., Warneke, C., de Gouw, J., Yee,
551 L., Seinfeld, J. H., Onasch, T. B., Herndon, S. C., Knighton, W. B., Cappa, C. D., Kleeman, M. J., Lim, C. Y.,
552 Kroll, J. H., Pierce, J. R., and Jathar, S. H.: Oxygenated Aromatic Compounds are Important Precursors of
553 Secondary Organic Aerosol in Biomass-Burning Emissions, Environ. Sci. Technol., 54, 8568-8579,
554 10.1021/acs.est.0c01345, 2020.
555 Alfarra, M. R., Prevot, A. S., Szidat, S., Sandradewi, J., Weimer, S., Lanz, V. A., Schreiber, D., Mohr, M., and
556 Baltensperger, U.: Identification of the mass spectral signature of organic aerosols from wood burning emissions,
557 Environmental science & technology, 41, 5770-5777, 2007.
558 Alves, V., Capanema, E., Chen, C.-L., and Gratzl, J.: Comparative studies on oxidation of lignin model
559 compounds with hydrogen peroxide using Mn (IV)-Me3TACN and Mn (IV)-Me4DTNE as catalyst, J. Mol. Catal.
560 A: Chem., 206, 37-51, 2003.
561 Andreae, M. O. and Merlet, P.: Emission of trace gases and aerosols from biomass burning, Global
562 biogeochemical cycles, 15, 955-966, 2001.
563 Asif, M.: Sustainability of timber, wood and bamboo in construction, in: Sustainability of construction materials,
564 Elsevier, 31-54, 2009.
565 Bailey, J., Gerasopoulos, E., Rojas-Rueda, D., and Benmarhnia, T.: Potential health and equity co-benefits related
566 to the mitigation policies reducing air pollution from residential wood burning in Athens, Greece, Journal of
567 Environmental Science and Health, Part A, 54, 1144-1151, 2019.
568 Balakrishnan, K., Ramaswamy, P., Sambandam, S., Thangavel, G., Ghosh, S., Johnson, P., Mukhopadhyay, K.,
569 Venugopal, V., and Thanasekaraan, V.: Air pollution from household solid fuel combustion in India: an overview
570 of exposure and health related information to inform health research priorities, Global health action, 4, 5638, 2011.
571 Bertrand, A., Stefenelli, G., Bruns, E. A., Pieber, S. M., Temime-Roussel, B., Slowik, J. G., Prévôt, A. S. H.,
572 Wortham, H., El Haddad, I., and Marchand, N.: Primary emissions and secondary aerosol production potential
573 from woodstoves for residential heating: Influence of the stove technology and combustion efficiency, Atmos.
574 Environ., 169, 65-79, 10.1016/j.atmosenv.2017.09.005, 2017.
575 Bhattu, D., Zotter, P., Zhou, J., Stefenelli, G., Klein, F., Bertrand, A., Temime-Roussel, B., Marchand, N., Slowik,
576 J. G., Baltensperger, U., Prevot, A. S. H., Nussbaumer, T., El Haddad, I., and Dommen, J.: Effect of Stove
577 Technology and Combustion Conditions on Gas and Particulate Emissions from Residential Biomass Combustion,
578 Environ. Sci. Technol., 53, 2209-2219, 10.1021/acs.est.8b05020, 2019.
579 Bruns, E. A., El Haddad, I., Slowik, J. G., Kilic, D., Klein, F., Baltensperger, U., and Prevot, A. S.: Identification
580 of significant precursor gases of secondary organic aerosols from residential wood combustion, Sci Rep, 6, 27881,
581 10.1038/srep27881, 2016.
582 Bruns, E. A., Slowik, J. G., El Haddad, I., Kilic, D., Klein, F., Dommen, J., Temime-Roussel, B., Marchand, N.,
583 Baltensperger, U., and Prévôt, A. S. H.: Characterization of gas-phase organics using proton transfer reaction
584 time-of-flight mass spectrometry: fresh and aged residential wood combustion emissions, Atmos. Chem. Phys.,
585 17, 705-720, 10.5194/acp-17-705-2017, 2017.
586 Burling, I., Yokelson, R. J., Griffith, D. W., Johnson, T. J., Veres, P., Roberts, J., Warneke, C., Urbanski, S.,
587 Reardon, J., and Weise, D.: Laboratory measurements of trace gas emissions from biomass burning of fuel types
588 from the southeastern and southwestern United States, Atmos. Chem. Phys., 10, 11115-11130, 2010.
589 Canagaratna, M. R., Jimenez, J. L., Kroll, J. H., Chen, Q., Kessler, S. H., Massoli, P., Hildebrandt Ruiz, L., Fortner,
590 E., Williams, L. R., Wilson, K. R., Surratt, J. D., Donahue, N. M., Jayne, J. T., and Worsnop, D. R.: Elemental
591 ratio measurements of organic compounds using aerosol mass spectrometry: characterization, improved
592 calibration, and implications, Atmos. Chem. Phys., 15, 253-272, 10.5194/acp-15-253-2015, 2015.
593 Carter, T. S., Heald, C. L., Kroll, J. H., Apel, E. C., Blake, D., Coggon, M., Edtbauer, A., Gkatzelis, G., Hornbrook,
594 R. S., and Peischl, J.: An improved representation of fire non-methane organic gases (NMOGs) in models:
595 emissions to reactivity, Atmos. Chem. Phys., 22, 12093-12111, 2022.
596 Chandramouli, C. and General, R.: Census of india 2011, Provisional Population Totals. New Delhi: Government
597 of India, 409-413, 2011.

598 Christian, T. J.: Comprehensive laboratory measurements of biomass-burning emissions: 2. First intercomparison
599 of open-path FTIR, PTR-MS, and GC-MS/FID/ECD, J. Geophys. Res., 109, 10.1029/2003jd003874, 2004.
600 Donahue, N. M., Robinson, A. L., and Pandis, S. N.: Atmospheric organic particulate matter: From smoke to
601 secondary organic aerosol, Atmos. Environ., 43, 94-106, 2009.
602 Donahue, N. M., Robinson, A., Stanier, C., and Pandis, S.: Coupled partitioning, dilution, and chemical aging of
603 semivolatile organics, Environmental science & technology, 40, 2635-2643, 2006.
604 Font-Palma, C.: Methods for the Treatment of Cattle Manure—A Review, C, 5, 10.3390/c5020027, 2019.
605 Font, A., Ciupek, K., Butterfield, D., and Fuller, G.: Long-term trends in particulate matter from wood burning in
606 the United Kingdom: Dependence on weather and social factors, Environ. Pollut., 314, 120105, 2022.
607 Fourtziou, L., Liakakou, E., Stavroulas, I., Theodosi, C., Zarmpas, P., Psiloglou, B., Sciare, J., Maggos, T.,
608 Bairachtari, K., and Bougiatioti, A.: Multi-tracer approach to characterize domestic wood burning in Athens
609 (Greece) during wintertime, Atmos. Environ., 148, 89-101, 2017.
610 Greenberg, J., Friedli, H., Guenther, A., Hanson, D., Harley, P., and Karl, T.: Volatile organic emissions from the
611 distillation and pyrolysis of vegetation, Atmos. Chem. Phys., 6, 81-91, 2006.
612 Grieshop, A., Logue, J., Donahue, N., and Robinson, A.: Laboratory investigation of photochemical oxidation of
613 organic aerosol from wood fires 1: measurement and simulation of organic aerosol evolution, Atmos. Chem. Phys.,
614 9, 1263-1277, 2009.
615 Guo, J., Wu, H., Zhao, Z., Wang, J., and Liao, H.: Review on health impacts from domestic coal burning: emphasis
616 on endemic fluorosis in Guizhou Province, Southwest China, Reviews of Environmental Contamination and
617 Toxicology Volume 258, 1-25, 2021.
618 Hatch, L. E., Rivas-Ubach, A., Jen, C. N., Lipton, M., Goldstein, A. H., and Barsanti, K. C.: Measurements of
619 I/SVOCs in biomass-burning smoke using solid-phase extraction disks and two-dimensional gas chromatography,
620 Atmos. Chem. Phys., 18, 17801-17817, 2018.
621 Hatch, L. E., Yokelson, R. J., Stockwell, C. E., Veres, P. R., Simpson, I. J., Blake, D. R., Orlando, J. J., and
622 Barsanti, K. C.: Multi-instrument comparison and compilation of non-methane organic gas emissions from
623 biomass burning and implications for smoke-derived secondary organic aerosol precursors, Atmos. Chem. Phys.,
624 17, 1471-1489, 2017.
625 Hatch, L. E., Jen, C. N., Kreisberg, N. M., Selimovic, V., Yokelson, R. J., Stamatis, C., York, R. A., Foster, D.,
626 Stephens, S. L., and Goldstein, A. H.: Highly speciated measurements of terpenoids emitted from laboratory and
627 mixed-conifer forest prescribed fires, Environmental Science & Technology, 53, 9418-9428, 2019.
628 He, C., Murray, F., and Lyons, T.: Seasonal variations in monoterpene emissions from Eucalyptus species,
629 Chemosphere-Global change science, 2, 65-76, 2000.
630 Hellén, H., Tykkä, T., and Hakola, H.: Importance of monoterpenes and isoprene in urban air in northern Europe,
631 Atmos. Environ., 59, 59-66, 10.1016/j.atmosenv.2012.04.049, 2012.
632 Hill Bembenic, M. A.: The chemistry of subcritical water reactions of a hardwood derived lignin and lignin model
633 compounds with nitrogen, hydrogen, carbon monoxide and carbon dioxide, 2011.
634 Hodzic, A., Jimenez, J. L., Madronich, S., Canagaratna, M. R., DeCarlo, P. F., Kleinman, L., and Fast, J.:
635 Modeling organic aerosols in a megacity: potential contribution of semi-volatile and intermediate volatility
636 primary organic compounds to secondary organic aerosol formation, Atmos. Chem. Phys., 10, 5491-5514,
637 10.5194/acp-10-5491-2010, 2010.
638 Huang, W., Li, H., Sarnela, N., Heikkinen, L., Tham, Y. J., Mikkilä, J., Thomas, S. J., Donahue, N. M., Kulmala,
639 M., and Bianchi, F.: Measurement report: Molecular composition and volatility of gaseous organic compounds in
640 a boreal forest – from volatile organic compounds to highly oxygenated organic molecules, Atmos. Chem. Phys.,
641 21, 8961-8977, 10.5194/acp-21-8961-2021, 2021.
642 Isaacman-VanWertz, G. and Aumont, B.: Impact of organic molecular structure on the estimation of
643 atmospherically relevant physicochemical parameters, Atmos. Chem. Phys., 21, 6541-6563, 10.5194/acp-21-
644 6541-2021, 2021.

645 Jin, L., Permar, W., Selimovic, V., Ketcherside, D., Yokelson, R. J., Hornbrook, R. S., Apel, E. C., Ku, I.-T.,
646 Collett Jr, J. L., and Sullivan, A. P.: Constraining emissions of volatile organic compounds from western US
647 wildfires with WE-CAN and FIREX-AQ airborne observations, Atmos. Chem. Phys., 23, 5969-5991, 2023.
648 Kalogridis, A.-C., Vratolis, S., Liakakou, E., Gerasopoulos, E., Mihalopoulos, N., and Eleftheriadis, K.:
649 Assessment of wood burning versus fossil fuel contribution to wintertime black carbon and carbon monoxide
650 concentrations in Athens, Greece, Atmos. Chem. Phys., 18, 10219-10236, 2018.
651 Keller, R. G., Di Marino, D., Blindert, M., and Wessling, M.: Hydrotropic solutions enable homogeneous fenton
652 treatment of lignin, Industrial & Engineering Chemistry Research, 59, 4229-4238, 2020.
653 Klein, F., Pieber, S. M., Ni, H., Stefenelli, G., Bertrand, A., Kilic, D., Pospisilova, V., Temime-Roussel, B.,
654 Marchand, N., El Haddad, I., Slowik, J. G., Baltensperger, U., Cao, J., Huang, R. J., and Prevot, A. S. H.:
655 Characterization of Gas-Phase Organics Using Proton Transfer Reaction Time-of-Flight Mass Spectrometry:
656 Residential Coal Combustion, Environ. Sci. Technol., 52, 2612-2617, 10.1021/acs.est.7b03960, 2018.
657 Koss, A. R., Sekimoto, K., Gilman, J. B., Selimovic, V., Coggon, M. M., Zarzana, K. J., Yuan, B., Lerner, B. M.,
658 Brown, S. S., and Jimenez, J. L.: Non-methane organic gas emissions from biomass burning: identification,
659 quantification, and emission factors from PTR-ToF during the FIREX 2016 laboratory experiment, Atmos. Chem.
660 Phys., 18, 3299-3319, 2018.
661 Krechmer, J., Lopez-Hilfiker, F., Koss, A., Hutterli, M., Stoermer, C., Deming, B., Kimmel, J., Warneke, C.,
662 Holzinger, R., Jayne, J., Worsnop, D., Fuhrer, K., Gonin, M., and de Gouw, J.: Evaluation of a New Reagent-Ion
663 Source and Focusing Ion-Molecule Reactor for Use in Proton-Transfer-Reaction Mass Spectrometry, Anal. Chem.,
664 90, 12011-12018, 10.1021/acs.analchem.8b02641, 2018.
665 Kumar, V., Slowik, J. G., Baltensperger, U., Prevot, A. S. H., and Bell, D. M.: Time-Resolved Molecular
666 Characterization of Secondary Organic Aerosol Formed from OH and NO(3) Radical Initiated Oxidation of a
667 Mixture of Aromatic Precursors, Environ. Sci. Technol., 57, 11572-11582, 10.1021/acs.est.3c00225, 2023.
668 Li, H., Riva, M., Rantala, P., Heikkinen, L., Daellenbach, K., Krechmer, J. E., Flaud, P.-M., Worsnop, D., Kulmala,
669 M., Villenave, E., Perraudin, E., Ehn, M., and Bianchi, F.: Terpenes and their oxidation products in the French
670 Landes forest: insights from Vocus PTR-TOF measurements, Atmos. Chem. Phys., 20, 1941-1959, 10.5194/acp-
671 20-1941-2020, 2020.
672 Li, K., Zhang, J., Bell, D. M., Wang, T., Lamkaddam, H., Cui, T., Qi, L., Surdu, M., Wang, D., Du, L., Haddad,
673 I. E., Slowik, J. G., and Prevot, A. S. H.: Uncovering the dominant contribution of intermediate volatility
674 compounds in secondary organic aerosol formation from biomass-burning emissions, National Science Review,
675 10.1093/nsr/nwae014, 2024.
676 Li, X., Wang, S., Duan, L., Hao, J., Li, C., Chen, Y., and Yang, L.: Particulate and Trace Gas Emissions from
677 Open Burning of Wheat Straw and Corn Stover in China, Environ. Sci. Technol., 41, 6052-6058,
678 10.1021/es0705137, 2007.
679 Li, Y., Pöschl, U., and Shiraiwa, M.: Molecular corridors and parameterizations of volatility in the chemical
680 evolution of organic aerosols, Atmos. Chem. Phys., 16, 3327-3344, 10.5194/acp-16-3327-2016, 2016.
681 Liu, C., Zhang, C., Mu, Y., Liu, J., and Zhang, Y.: Emission of volatile organic compounds from domestic coal
682 stove with the actual alternation of flaming and smoldering combustion processes, Environ. Pollut., 221, 385-391,
683 10.1016/j.envpol.2016.11.089, 2017.
684 Liu, Y., Shao, M., Fu, L., Lu, S., Zeng, L., and Tang, D.: Source profiles of volatile organic compounds (VOCs)
685 measured in China: Part I, Atmos. Environ., 42, 6247-6260, 10.1016/j.atmosenv.2008.01.070, 2008.
686 Liu, Y., Liao, B., Guo, W., Fu, Y., Sun, W., Fu, Y., Wang, D., and Kang, H.: Study on Separation and Purification
687 of Chemical Components of Dichloromethane from Pine Needle Extract, IOP Conference Series: Earth and
688 Environmental Science, 032039,
689 Loebel Roson, M., Duruisseau-Kuntz, R., Wang, M., Klimchuk, K., Abel, R. J., Harynuk, J. J., and Zhao, R.:
690 Chemical Characterization of Emissions Arising from Solid Fuel Combustion—Contrasting Wood and Cow Dung
691 Burning, ACS Earth and Space Chemistry, 5, 2925-2937, 10.1021/acsearthspacechem.1c00268, 2021.

692 Ma, Y. and Hays, M. D.: Thermal extraction–two-dimensional gas chromatography–mass spectrometry with
693 heart-cutting for nitrogen heterocyclics in biomass burning aerosols, J. Chromatogr. A, 1200, 228-234, 2008.
694 Majluf, F. Y., Krechmer, J. E., Daube, C., Knighton, W. B., Dyroff, C., Lambe, A. T., Fortner, E. C., Yacovitch,
695 T. I., Roscioli, J. R., Herndon, S. C., Worsnop, D. R., and Canagaratna, M. R.: Mobile Near-Field Measurements
696 of Biomass Burning Volatile Organic Compounds: Emission Ratios and Factor Analysis, Environmental Science
697 & Technology Letters, 9, 383-390, 10.1021/acs.estlett.2c00194, 2022.
698 Mann, H. B. and Whitney, D. R.: On a test of whether one of two random variables is stochastically larger than
699 the other, Annals of Mathematical Statistics, 18, 50-60, 10.1214/aoms/1177730491, 1947.
700 Mastral, A. M. and Callen, M. S.: A review on polycyclic aromatic hydrocarbon (PAH) emissions from energy
701 generation, Environmental Science & Technology, 34, 3051-3057, 2000.
702 Ni, H., Huang, R.-J., Pieber, S. M., Corbin, J. C., Stefenelli, G., Pospisilova, V., Klein, F., Gysel-Beer, M., Yang,
703 L., and Baltensperger, U.: Brown carbon in primary and aged coal combustion emission, Environmental Science
704 & Technology, 55, 5701-5710, 2021.
705 Noe, S. M., Hüve, K., Niinemets, Ü., and Copolovici, L.: Seasonal variation in vertical volatile compounds air
706 concentrations within a remote hemiboreal mixed forest, Atmos. Chem. Phys., 12, 3909-3926, 10.5194/acp-12-
707 3909-2012, 2012.
708 Oberschelp, C., Pfister, S., Raptis, C., and Hellweg, S.: Global emission hotspots of coal power generation, Nature
709 Sustainability, 2, 113-121, 2019.
710 Pallozzi, E., Lusini, I., Cherubini, L., Hajiaghayeva, R. A., Ciccioli, P., and Calfapietra, C.: Differences between
711 a deciduous and a conifer tree species in gaseous and particulate emissions from biomass burning, Environ. Pollut.,
712 234, 457-467, 10.1016/j.envpol.2017.11.080, 2018.
713 Permar, W., Wang, Q., Selimovic, V., Wielgasz, C., Yokelson, R. J., Hornbrook, R. S., Hills, A. J., Apel, E. C.,
714 Ku, I. T., and Zhou, Y.: Emissions of trace organic gases from Western US wildfires based on WE-CAN aircraft
715 measurements, Journal of Geophysical Research: Atmospheres, 126, e2020JD033838, 2021.
716 Ren, Q. and Zhao, C.: Evolution of fuel-N in gas phase during biomass pyrolysis, Renewable and Sustainable
717 Energy Reviews, 50, 408-418, 2015.
718 Riva, M., Rantala, P., Krechmer, J. E., Peräkylä, O., Zhang, Y., Heikkinen, L., Garmash, O., Yan, C., Kulmala,
719 M., Worsnop, D., and Ehn, M.: Evaluating the performance of five different chemical ionization techniques for
720 detecting gaseous oxygenated organic species, Atmospheric Measurement Techniques, 12, 2403-2421,
721 10.5194/amt-12-2403-2019, 2019.
722 Robinson, A. L., Donahue, N. M., Shrivastava, M. K., Weitkamp, E. A., Sage, A. M., Grieshop, A. P., Lane, T.
723 E., Pierce, J. R., and Pandis, S. N.: Rethinking organic aerosols: Semivolatile emissions and photochemical aging,
724 Sci, 315, 1259-1262, 2007.
725 Sarkar, C., Sinha, V., Kumar, V., Rupakheti, M., Panday, A., Mahata, K. S., Rupakheti, D., Kathayat, B., and
726 Lawrence, M. G.: Overview of VOC emissions and chemistry from PTR-TOF-MS measurements during the
727 SusKat-ABC campaign: high acetaldehyde, isoprene and isocyanic acid in wintertime air of the Kathmandu
728 Valley, Atmos. Chem. Phys., 16, 3979-4003, 10.5194/acp-16-3979-2016, 2016.
729 Schneider, J., Weimer, S., Drewnick, F., Borrmann, S., Helas, G., Gwaze, P., Schmid, O., Andreae, M., and
730 Kirchner, U.: Mass spectrometric analysis and aerodynamic properties of various types of combustion-related
731 aerosol particles, Int. J. Mass spectrom., 258, 37-49, 2006.
732 Sengpiel, R., Di Marino, D., Blindert, M., and Wessling, M.: 7 Hydrotropic solutions for Fenton depolymerization
733 of lignin, Extraction and Electrochemical Valorization of Lignin in Novel Electrolytes, 107, 2019.
734 Simoneit, B. R., Rogge, W., Mazurek, M., Standley, L., Hildemann, L., and Cass, G.: Lignin pyrolysis products,
735 lignans, and resin acids as specific tracers of plant classes in emissions from biomass combustion, Environmental
736 science & technology, 27, 2533-2541, 1993.
737 Stala-Szlugaj, K.: The demand for hard coal for households in Poland and the anti-smog bill, Archives of Mining
738 Sciences, 63, 701-711, 2018.

739 Stewart, G. J., Acton, W. J. F., Nelson, B. S., Vaughan, A. R., Hopkins, J. R., Arya, R., Mondal, A., Jangirh, R.,
740 Ahlawat, S., Yadav, L., Sharma, S. K., Dunmore, R. E., Yunus, S. S. M., Hewitt, C. N., Nemitz, E., Mullinger,
741 N., Gadi, R., Sahu, L. K., Tripathi, N., Rickard, A. R., Lee, J. D., Mandal, T. K., and Hamilton, J. F.: Emissions
742 of non-methane volatile organic compounds from combustion of domestic fuels in Delhi, India, Atmos. Chem.
743 Phys., 21, 2383-2406, 10.5194/acp-21-2383-2021, 2021a.
744 Stewart, G. J., Nelson, B. S., Acton, W. J. F., Vaughan, A. R., Farren, N. J., Hopkins, J. R., Ward, M. W., Swift,
745 S. J., Arya, R., Mondal, A., Jangirh, R., Ahlawat, S., Yadav, L., Sharma, S. K., Yunus, S. S. M., Hewitt, C. N.,
746 Nemitz, E., Mullinger, N., Gadi, R., Sahu, L. K., Tripathi, N., Rickard, A. R., Lee, J. D., Mandal, T. K., and
747 Hamilton, J. F.: Emissions of intermediate-volatility and semi-volatile organic compounds from domestic fuels
748 used in Delhi, India, Atmos. Chem. Phys., 21, 2407-2426, 10.5194/acp-21-2407-2021, 2021b.
749 Stockwell, C. E., Veres, P. R., Williams, J., and Yokelson, R. J.: Characterization of biomass burning emissions
750 from cooking fires, peat, crop residue, and other fuels with high-resolution proton-transfer-reaction time-of-flight
751 mass spectrometry, Atmos. Chem. Phys., 15, 845-865, 10.5194/acp-15-845-2015, 2015.
752 Tao, S., Ru, M., Du, W., Zhu, X., Zhong, Q., Li, B., Shen, G., Pan, X., Meng, W., and Chen, Y.: Quantifying the
753 rural residential energy transition in China from 1992 to 2012 through a representative national survey, Nature
754 Energy, 3, 567-573, 2018.
755 Tkacik, D. S., Robinson, E. S., Ahern, A., Saleh, R., Stockwell, C., Veres, P., Simpson, I. J., Meinardi, S., Blake,
756 D. R., Yokelson, R. J., Presto, A. A., Sullivan, R. C., Donahue, N. M., and Robinson, A. L.: A dual-chamber
757 method for quantifying the effects of atmospheric perturbations on secondary organic aerosol formation from
758 biomass burning emissions, Journal of Geophysical Research: Atmospheres, 122, 6043-6058,
759 10.1002/2016jd025784, 2017.
760 Wang, D. S., Lee, C. P., Krechmer, J. E., Majluf, F., Tong, Y., Canagaratna, M. R., Schmale, J., Prévôt, A. S. H.,
761 Baltensperger, U., Dommen, J., El Haddad, I., Slowik, J. G., and Bell, D. M.: Constraining the response factors
762 of an extractive electrospray ionization mass spectrometer for near-molecular aerosol speciation, Atmospheric
763 Measurement Techniques, 14, 6955-6972, 10.5194/amt-14-6955-2021, 2021.
764 Ward, D. and Radke, L.: Emissions measurements from vegetation fires: A comparative evaluation of methods
765 and results, Fire in the Environment: The Ecological, Atmospheric and Climatic Importance of Vegetation Fires,
766 13, 53-76, 1993.
767 Warneke, C., Roberts, J. M., Veres, P., Gilman, J., Kuster, W. C., Burling, I., Yokelson, R., and de Gouw, J. A.:
768 VOC identification and inter-comparison from laboratory biomass burning using PTR-MS and PIT-MS, Int. J.
769 Mass spectrom., 303, 6-14, 10.1016/j.ijms.2010.12.002, 2011.
770 Weber, K. T. and Yadav, R.: Spatiotemporal trends in wildfires across the Western United States (1950–2019),
771 Remote Sensing, 12, 2959, 2020.
772 Weimer, S., Alfarra, M. R., Schreiber, D., Mohr, M., Prévôt, A. S. H., and Baltensperger, U.: Organic aerosol
773 mass spectral signatures from wood-burning emissions: Influence of burning conditions and wood type, J.
774 Geophys. Res., 113, 10.1029/2007jd009309, 2008.
775 Wilcoxon, F.: Individual Comparisons by Ranking Methods, Biometrics Bulletin, 1, 80-83, 10.2307/3001968,
776 1945.
777 Williams, A. P., Allen, C. D., Macalady, A. K., Griffin, D., Woodhouse, C., Meko, D. M., Swetnam, T. W.,
778 Rauscher, S. A., Seager, R., and Grissino-Mayer, H. D.: Temperature as a potent driver of regional forest drought
779 stress and tree mortality, 2012.
780 Wu, D., Zheng, H., Li, Q., Jin, L., Lyu, R., Ding, X., Huo, Y., Zhao, B., Jiang, J., and Chen, J.: Toxic potency-
781 adjusted control of air pollution for solid fuel combustion, Nature Energy, 7, 194-202, 2022.
782 Yuan, B., Koss, A. R., Warneke, C., Coggon, M., Sekimoto, K., and de Gouw, J. A.: Proton-Transfer-Reaction
783 Mass Spectrometry: Applications in Atmospheric Sciences, Chem Rev, 117, 13187-13229,
784 10.1021/acs.chemrev.7b00325, 2017.
785 Zhang, J. and Smith, K. R.: Household air pollution from coal and biomass fuels in China: measurements, health
786 impacts, and interventions, Environ. Health Perspect., 115, 848-855, 2007.

787   Zhang, J., Li, K., Wang, T., Gammelsæter, E., Cheung, R. K., Surdu, M., Bogler, S., Bhattu, D., Wang, D. S., and
788   Cui, T.: Bulk and molecular-level composition of primary organic aerosol from wood, straw, cow dung, and
789   plastic burning, Atmos. Chem. Phys., 23, 14561-14576, 2023.

790   Zhang, J., Smith, K., Ma, Y., Ye, S., Jiang, F., Qi, W., Liu, P., Khalil, M., Rasmussen, R., and Thorneloe, S.:
791   Greenhouse gases and other airborne pollutants from household stoves in China: a database for emission factors,
792   Atmos. Environ., 34, 4537-4549, 2000.

793   Zhang, X., Xu, J., Zhai, L., and Zhao, W.: Characterization of Aerosol Properties from the Burning Emissions of
794   Typical Residential Fuels on the Tibetan Plateau, Environ. Sci. Technol., 56, 14296-14305,
795   10.1021/acs.est.2c04211, 2022.

796   Zhao, B., Wang, S., Donahue, N. M., Jathar, S. H., Huang, X., Wu, W., Hao, J., and Robinson, A. L.: Quantifying
797   the effect of organic aerosol aging and intermediate-volatility emissions on regional-scale aerosol pollution in
798   China, Scientific reports, 6, 28815, 2016.

799   Zhao, N., Li, B., Ahmad, R., Ding, F., Zhou, Y., Li, G., Zayan, A. M. I., and Dong, R.: Dynamic relationships
800   between real-time fuel moisture content and combustion-emission-performance characteristics of wood pellets in
801   a top-lit updraft cookstove, Case Studies in Thermal Engineering, 28, 10.1016/j.csite.2021.101484, 2021.

802